Langmuir Article

pubs.acs.org/Langmuir

Monodisperse Cobalt Ferrite Nanomagnets with Uniform Silica Coatings

Qiu Dai,[†] Michelle Lam,[†] Sally Swanson,[†] Rui-Hui Rachel Yu,[†] Delia J. Milliron,[‡] Teya Topuria,[†] Pierre-Olivier Jubert,*[,†] and Alshakim Nelson*[,†]

[†]*IBM Almaden Research Center, 650 Harry Road, San Jose, California 95120, United States, and* [‡]*The Molecular Foundry, Lawrence Berkeley National Laboratory, 1 Cyclotron Road, MS 67R4110, Berkeley, California 94611, United States*

Received July 30, 2010. Revised Manuscript Received September 30, 2010

Ferro- and ferrimagnetic nanoparticles are difficult to manipulate in solution as a consequence of the formation of magnetically induced nanoparticle aggregates, which hamper the utility of these particles for applications ranging from data storage to bionanotechnology. Nonmagnetic shells that encapsulate these magnetic particles can reduce the interparticle magnetic interactions and improve the dispersibility of the nanoparticles in solution. A route to create uniform silica shells around individual cobalt ferrite nanoparticles—which uses poly(acrylic acid) to bind to the nanoparticle surface and inhibit nanoparticle aggregation prior to the addition of a silica precursor—was developed. In the absence of the poly(acrylic acid) the cobalt ferrite nanoparticles irreversibly aggregated during the silica shell formation. The thickness of the silica shell around the core−shell nanoparticles could be controlled in order to tune the interparticle magnetic coupling as well as inhibit magnetically induced nanoparticle aggregation. These ferrimagnetic core−silica shell structures form stable dispersion in polar solvents such as EtOH and water, which is critical for enabling technologies that require the assembly or derivatization of ferrimagnetic particles in solution.

Introduction

Magnetic nanoparticles (MNPs) represent a set of unique building blocks whose size and composition are tunable to meet the requirements for a range of applications including magnetic fluids,[1] catalysis,[2] data storage,[3] biomedicine,[4] and toxic waste remediation.[5] While single domain MNPs can maintain ferromagnetic or ferrimagnetic properties that are suitable for magnetic recording technologies, the particles become superparamagnetic as their diameter continues to decrease. In contrast to superparamagnetic nanoparticles (SPMNPs), ferri- and ferromagnetic nanoparticles (FMNPs) have a stable magnetic dipole moment at a given temperature in the absence of an external magnetic field. Thus, unlike SPMNPs, FMNPs are subject to strong interparticle magnetic coupling interactions or magnetically induced particle aggregation even in the absence of an external field.[6] A signficant challenge to utilizing ferri- and ferromagnetic MNPs for materials applications is the inherent aggregation of particles which takes place as a result of interparticle magnetic attractive forces. Solution-based processing of FMNPs is appealing—for instance, for magnetic recording applications—yet the formation of high-quality dispersions is difficult, motivating the development of new strategies to moderate inteparticle forces.

Surface coating of FMNPs with a nonmagnetic shell represents an appealing route to reduce interparticle magnetic forces and minimize their aggregation.[7a−e] For example, Pyun and co-workers demonstrated that core−shell structures comprised of a ferromagnetic core and a nonmagnetic polystyrene corona afforded stable colloids in a variety of organic solvents over a period of several months. The core−shell composites assembled into one-dimensional magnetic structures, wherein the polymer-coated cobalt nanoparticles were organized into extended chainlike structures spanning several micrometers in length.

Alternatively, magnetic core−shell structures with a silica or an organosilicate corona provide a means to surround magnetic nanoparticles with a robust nonmagnetic coating. Strategies that use silica shells, including those that employ layer-by-layer assemblies to form silica shells,[7f−h] offer several advantages, including (1) the ability to control the thickness of the shell and thereby control the spacing between the MNPs and (2) a highly robust inorganic coating that can be covalently functionalized at the periphery with organic substituents. Protocols for the encapsulation of individual SPMNPs (at room temperature) with a silica shell have been reported;[8] however, these methods are not suitable for FMNPs (at room temperature). The encapsulation of FMNPs with a discrete silica shell is hampered by the strong magnetic attractive forces between nanoparticles. Aggregation of the particles—both prior to and during the silica growth step—leads to the formation of nonuniform shells around particle clusters which hinders the production of monodisperse samples. Korgel and co-workers reported a strategy that allowed the formation of uniform silica shells

*Corresponding authors. E-mail: alshak@us.ibm.com (A.N.), pjubert@us.ibm.com (P.-O.J.).

(1) Zahn, M. *J. Nanopart. Res.* **2001**, *3*, 73.
(2) Yoon, T. J.; Lee, W.; Oh, Y. S.; Lee, J. K. *New J. Chem.* **2003**, *27*, 227.
(3) Ross, C. A. *Annu. Rev. Mater. Res.* **2001**, *31*, 203.
(4) Ito, A.; Shinkai, M.; Honda, H.; Kobayashi, T. *J. Biosci. Bioeng.* **2005**, *1*, 1.
(5) Liu, W. T. *J. Biosci. Bioeng.* **2006**, *102*, 1.
(6) (a) Pyun, J. *Polym. Rev.* **2007**, *47*, 231.(b) Varadan, V. K.; Chen, L.; Xie, J. *Nanomedicine: Design and Applications of Magnetic Nanomaterials, Nanosensors and Nanosystems*; John Wiley & Sons Ltd.: New York, 2008.
(7) (a) Keng, Y.; Shim, I.; Korth, B. D.; Douglas, J. F.; Pyun, J. *ACS Nano* **2007**, *1*, 279. (b) Korth, B. D.; Keng, P. K.; Shim, I.; Bowles, S. E.; Tang, C.; Kowalewski, T.; Nebesny, K. W.; Pyun, J. *J. Am. Chem. Soc.* **2006**, *128*, 6562. (c) Vestal, C. R.; Zhang, Z. J. *J. Am. Chem. Soc.* **2002**, *124*, 14312. (d) Wang, Y.; Wong, J. F.; Teng, X.; Lin, X. Z.; Yang, H. *Nano Lett.* **2003**, *3*, 1555. (e) Amstad, E.; Gillich, T.; Bilecka, I.; Textor, M.; Reimhult, E. *Nano Lett.* **2009**, *9*, 4042. (f) Caruso, F.; Lichtenfeld, H.; Giersig, M.; Mohwald, H. *J. Am. Chem. Soc.* **1998**, *120*, 8523. (g) Caruso, F.; Caruso, R. A.; Mohwald, H. *Science* **1998**, *282*, 1111. (h) Aliev, F. G.; Correa-Duarte, M. A.; Mamedov, A.; Ostrander, J. W.; Giersig, M.; Liz-Marzan, L. M.; Kotov, N. *Adv. Mater.* **1999**, *11*, 1006.
(8) (a) Yi, D. K.; Selvan, S. T.; Lee, S. S.; Papaefthymiou, G. C.; Kundaliya, D.; Ying, J. Y. *J. Am. Chem. Soc.* **2005**, *127*, 4990. (b) Wang, J.; Zhang, K.; Zhu, Y. *J. Nanosci. Nanotechnol.* **2005**, *5*, 772. (c) Bonini, M.; Wiedenmann, A.; Baglioni, P. *Mater. Sci. Eng., C* **2006**, *26*, 745. (d) Vestal, C. R.; Zhang, Z. J. *Nano Lett.* **2003**, *3*, 1739.

around individual ferromagnetic FePt MNPs without magnetically induced aggregation of the particles.[9] In this process, the silica shell was first grown around superparamagnetic FePt particles (in their disordered fcc alloy phase) prior to thermally annealing to transform the FePt into its ferromagnetic intermetallic phase. This process is specific for FePt-containing core−shell structures and is not necessarily suitable for other FMNPs of other compositions.

Among ferrite materials,[10,11] ferrimagnetic cobalt ferrite ($CoFe_2O_4$) nanoparticles with an inverse spinel structure are of particular interest as a consequence of their ease of synthesis via colloidal methods, remarkable chemical stability, excellent mechanical strength, high magnetocrystalline anisotropy, and moderate saturation magnetization.[12] The solution phase synthesis of $CoFe_2O_4$ MNPs with uniform size and morphology has progressed significantly during the past decade.[11,13] One of the most commonly used methods is the thermal decomposition of $Fe(acac)_3$ and $Co(acac)_2$ precursors in the presence of oleic acid surfactant in a high boiling point solvent such as benzyl ether. The magnetic properties of $CoFe_2O_4$ MNPs can be tuned from superparamagnetic to ferrimagnetic at room temperature by increasing the diameter of the MNPs.[14] The as-synthesized $CoFe_2O_4$ MNPs are protected by oleic acid surfactants on the surface, which afford the nanoparticles dispersibility in nonpolar solvents such as hexane. However, in our experience, small molecule surfactants are not suitable for stabilizing $CoFe_2O_4$ MNPs which are ferrimagnetic ($> \sim 16$ nm) at room temperature. Over time, the ferrimagnetic particles irreversibly aggregate and ultimately precipitate from solution as a result of the strong magnetic forces which exist between neighboring MNPs. Herein, we describe a method to construct uniform silica shells around individual ferrimagnetic $CoFe_2O_4$ nanoparticles which effectively inhibit particle aggregation and moderate the magnetic coupling interaction between neighboring nanoparticles.

Experimental Section

Materials. Cobalt(II) acetylacetonate (97%), iron(III) acetylacetonate (99.99%), oleic acid (90%), oleylamine (90%), 1,2-hexadecanediol (90%), poly(acrylic acid) (MW = 1800), benzyl ether (99%), tetraethyl orthosilicate (99.99%), and ammonium hydroxide (30 wt %) were obtained from Sigma-Aldrich. Hexane, ethanol, and tetrahydrofuran were purchased from J.T. Baker. All the chemicals were used as received without any further purification.

Synthesis of 6 nm Oleic Acid-Protected $CoFe_2O_4$ Nanoparticles. The $CoFe_2O_4$ MNPs were prepared using an adaptation of the procedure reported by Sun et al.[11] Briefly, 2 mmol of $Fe(acac)_3$, 1 mmol of $Co(acac)_2$, 10 mmol of 1,2-hexadecanediol, 6 mmol of oleic acid, 6 mmol of oleylamine, and 20 mL of benzyl ether were combined and mechanically stirred under a flow of N_2. The mixture was heated to 200 °C for 2 h and then, under a blanket of N_2, heated to reflux (~300 °C) for 1 h. The black mixture was cooled to room temperature by removing the heat sources. Under ambient conditions, 40 mL of ethanol was added to the mixture, and a black material was precipitated and separated via centrifugation at 6000 rpm for 10 min. The supernatant was decanted, and the black precipitate was dissolved in hexane with 0.1% oleic acid. The mixture was centrifuged at 6000 rpm for 10 min, and the supernatant was decanted again. The product was then precipitated with ethanol, centrifuged and decanted to remove the solvent, and then dried in vacuum overnight. The average diameter of the $CoFe_2O_4$ nanoparticles was 6 nm with a narrow size distribution as determined by TEM.

Synthesis of 18 nm Oleic Acid-Protected $CoFe_2O_4$ Nanoparticles. The as-synthesized 6 nm $CoFe_2O_4$ nanoparticles were further used as seeds to grow larger particles. Typically, 2 mmol of $Fe(acac)_3$, 1 mmol of $Co(acac)_2$, 10 mmol of 1,2-hexadecanediol, 2 mmol of oleic acid, 2 mmol of oleylamine, and 20 mL of benzyl ether were mixed and mechanically stirred under a flow of N_2. A solution of the synthesized 6 nm $CoFe_2O_4$ MNP hexane solution (6 mL, 15 mg/mL) was added to the reaction. The mixture was first heated to 100 °C for 30 min to remove hexane and then increased to 200 °C for 1 h. Under a blanket of N_2, the mixture was further heated to 300 °C for 30 min. Following the same workup procedures as above, the monodispersed $CoFe_2O_4$ nanoparticles with a diameter of 15 nm were obtained. The particle growth procedure was repeated one additional time using the 15 nm MNPs as seeds to prepare 18 nm monodisperse $CoFe_2O_4$ MNPs.

PAA Coating of Oleic Acid-Protected 18 nm $CoFe_2O_4$ MNPs. In a glass vial under ambient conditions, 1 mL of PAA (MW = 1800 g/mol) solution in THF (10 mg/mL) was added to a hexane dispersion of the 18 nm fresh prepared $CoFe_2O_4$ MNPs (10 mg in 10 mL). The mixture was shaken for 2 h with occasional sonication. The modified particles were separated with a magnet, and the solvent was decanted. The particles were washed three times with hexane and methanol to remove the free oleic acid and excess PAA polymers. The washed particles were dispersed in aqueous solution by ionizing the carboxylic groups with a dilute NaOH solution.

Silica Coating of PAA-Modified $CoFe_2O_4$ MNPs. The PAA-modified $CoFe_2O_4$ MNPs in aqueous solution (1.5 mL) was diluted with ethanol (10 mL) and ammonium hydroxide (30 wt %, 400 μL) with vigorous mechanical stirring. A TEOS solution in ethanol (200 μL, 10 mM) was added to the mixture every 2 h until the total amount of TEOS solution reached 1 mL. After obtaining the desired size, the silica-coated $CoFe_2O_4$ MNPs were collected by magnetic separation, washed with ethanol three times, and finally dispersed in ethanol for further characterization.

Characterization Methods. Fourier transform infrared spectra (FT-IR spectra) of the $CoFe_2O_4$ MNPs were recorded on a Thermo Nicolet NEXUS 670 FT-IR. Thermal gravimetric analysis (TGA) was performed under a nitrogen atmosphere at a heating rate of 10 °C/min using a Perkin-Elmer TGS-2 instrument. Transmission electron microscopy (TEM) images were recorded on a Philips CM12 TEM (120 kV). A drop of $CoFe_2O_4$ MNP solution was placed onto a carbon-coated copper grid and left to dry at room temperature. Magnetic measurements were carried out using an ADE Technologies DMS Model 10 vibrating sample magnetometer (VSM).

Results and Discussion

Monodisperse samples of $CoFe_2O_4$ nanoparticles were synthesized using an adapted version of the procedures reported by Sun and co-workers.[11] In this process, 6 nm diameter seed particles were first synthesized and then used to nucleate the formation of larger particles until the desired diameter was obtained (18 nm). Analysis of the 6 and 18 nm particles by vibrating sample magnetometry (VSM) at room temperature demonstrated that the samples were superparamagnetic and ferrimagnetic, respectively (Supporting Information Figure S1). The 18 nm ferrimagnetic particles behave as nanomagnets with, for a random assembly of these particles, a coercivity of 739 Oe at ambient temperature. The 6 nm particles can easily be encapsulated with uniform silica coatings (Figure 1a, see also Supporting Information Figure S2) using

(9) Lee, D. C.; Mikulec, F. V.; Pelaez, J. M.; Korgel, B. A. *J. Phys. Chem. B* **2006**, *110*, 11160.
(10) Gee, S. H.; Kong, Y. K.; Jeffers, F. J.; Park, M. H.; Sur, J. C.; Weatherspoon, C.; Nam, I. T. *IEEE Trans. Magn.* **2005**, *41*, 4353.
(11) Sun, S.; Zeng, H.; Robinson, D. B.; Raoux, S.; Rice, P. M.; Wang, S.; Li, G. *J. Am. Chem. Soc.* **2004**, *126*, 273.
(12) Ning, M.; Li, J.; Ong, C. K.; Wang, S. J. *J. Appl. Phys.* **2008**, *103*, 13911.
(13) (a) Rondinone, A. J.; Samia, A. C.; Zhang, Z. J. *J. Phys. Chem. B* **1999**, *103*, 6876. (b) Bao, N.; Shen, L.; An, W.; Padhan, P.; Turner, C. H.; Gupta, A. *Chem. Mater.* **2009**, *21*, 3458.
(14) Song, Q.; Zhang, Z. J. *J. Am. Chem. Soc.* **2004**, *126*, 6164.

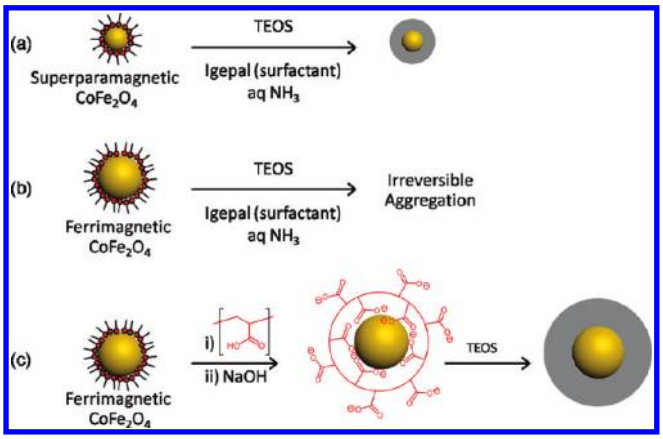

Figure 1. (a) Formation of silica shell around individual $CoFe_2O_4$ SPMNPs. (b) The same conditions used for the SPMNPs were not effective for encapsulating FMNPs with uniform silica shells. (c) Method used for encapsulating FMNPs with uniform silica shells by first reacting the particle surface with PAA and then exposing to TEOS.

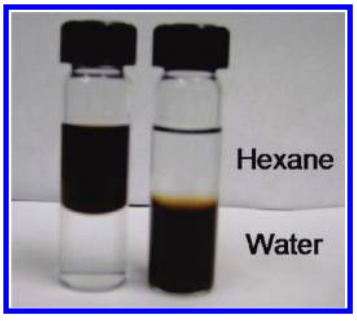

Figure 2. Image showing the change in solubility of the $CoFe_2O_4$ FMNPs before (left) and after (right) treatment with PAA. The top layer is hexane, and the bottom layer is water.

TEOS as the SiO_2 source in a reverse microemulsion process.[8d] However, under the same conditions, the larger ferrimagnetic nanoparticles immediately precipitated from the reaction mixture upon the addition of TEOS (Figure 1b). Magnetically induced aggregation likely occurs as the TEOS reacts with the particle surface and displaces the oleic acid surfactants.

In order to prevent the aggregation of the $CoFe_2O_4$ nanoparticles during the silica coating process, we employed a ligand exchange method that uses poly(acrylic acid) (PAA) to replace the oleic acid surfactants on the particle surface (Figure 1c). In a typical process, a hexane solution containing oleic acid-protected $CoFe_2O_4$ FMNPs was combined with a THF solution of PAA. The solution became turbid immediately, indicating the occurrence of the ligand exchange process. The oleic acid surfactants on the particle were replaced by carboxylic acid groups of the PAA chain, which bound the MNP surface in a multivalent manner. After washing the MNPs with copious amounts of hexane and methanol to remove the free oleic acid surfactant and residual unbound PAA, the hydrophilic PAA-modified $CoFe_2O_4$ nanoparticles were dispersed in an aqueous ethanol solution. The absence of any precipitation indicates successful ligand exchange of PAA for oleic acid on the particle surface. As shown in Figure 2, the $CoFe_2O_4$ FMNPs now have a hydrophilic surface and have phase transferred from hexane to water as a result of the exchange process. The aqueous solution of PAA-modified $CoFe_2O_4$ nanoparticles is stable when the pH value is above 7. No obvious change was observed after storing the sample for more than 3 months under ambient conditions. Compared to other reported ligand exchange processes,[15] this approach has a number of unique advantages. First, the PAA polymer chains bind to the nanoparticle surface through multiple anchoring points, providing a more robust surface adsorption than that achievable with a small molecule that has only one binding group. Second, the attached polymer chains are well suited to sterically stabilize FMNPs relative to small molecule surfactants. Third, the abundant uncoordinated acid groups on the PAA chain provide aqueous solubility.

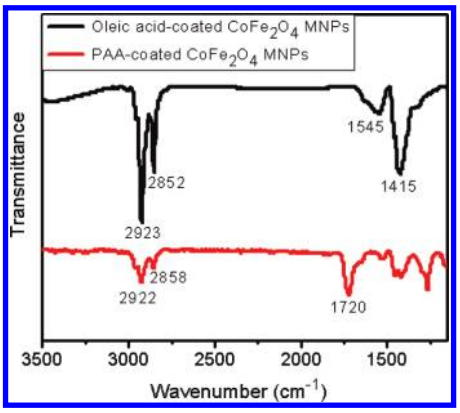

Figure 3. FT-IR spectra of $CoFe_2O_4$ MNPs (18 nm) before and after PAA modification.

Fourier transform infrared (FT-IR) spectroscopy was utilized to characterize the functional groups present on the particle surface after the PAA ligand exchange as shown in Figure 3. The oleic acid-protected $CoFe_2O_4$ FMNPs showed strong CH_2 bands at 2923 and 2852 cm^{-1} which are associated with the methylenes present in oleic acid. The bands at 1545 and 1415 cm^{-1} can be assigned to the antisymmetric and symmetric vibration modes of the carboxylate groups, indicating the adsorption of oleic acid onto the particle surface. A similar spectrum was observed when oleic acid surfactants were adsorbed onto iron oxide particle surfaces.[16] After the ligand exchange with PAA, a new band corresponding to the stretching mode of −COOH groups appears at 1720 cm^{-1}. In addition, the bands at 2922 and 2853 cm^{-1} associated with the oleic acid methylenes decreased after ligand exchange process. These observations strongly suggest that PAA chains were successfully attached onto the particle surface in place of oleic acid surfactants.

Thermogravimetric analysis (TGA) measurements were conducted (Figure 4) to determine quantitatively the PAA density adsorbed onto the particle surface. The oleic acid-protected $CoFe_2O_4$ MNPs show a strong primary mass loss at ~280 °C followed by a second transition for mass loss at 400 °C. The 13% total weight loss which spans from 200 to 550 °C is attributed to the desorption of oleic acid and is in agreement with the values reported in the literature.[15b] The TGA of the PAA-modified $CoFe_2O_4$ MNPs showed a mass loss of 25% in the same temperature range which is ascribed to the decomposition of PAA. With an average particle size of 18 nm and cobalt ferrite density of 5.15 g/cm^3, we can further estimate that the number of PAA chains attached to the surface was on average 1750 per nanoparticle.

(15) (a) Kraus, A.; Jainae, K.; Unob, F.; Sukpiron, N. *J. Colloid Interface Sci.* **2009**, *338*, 359. (b) Palma, R. D.; Peeters, S.; Baei, M. J.; Rul, H. V.; Bonrov, K.; Laureyn, W.; Mullens, J.; Borghs, G.; Maes, G. *Chem. Mater.* **2007**, *19*, 1821. (c) Robinson, D. B.; Persson, H. J.; Zeng, H.; Li, G.; Pourmand, N.; Sun, S.; Wang, S. *Langmuir* **2005**, *21*, 3096. (d) Wu, C. K.; Hultman, K. L.; O'Brien, S.; Koberstein, J. T. *J. Am. Chem. Soc.* **2008**, *130*, 3516–3520. (e) Pastoriza-Santos, I.; Perez-Juste, J.; Liz-Marzan, L. M. *Chem. Mater.* **2006**, *18*, 2465–2467.

(16) Zhang, T.; Ge, J.; Hu, Y.; Yin, Y. *Nano Lett.* **2007**, *7*, 3203.

TEM images further confirmed that the MNP core does not change after PAA ligand exchange. As shown in Figure 5a, the oleic acid-protected ferrimagnetic $CoFe_2O_4$ nanoparticles are spherical with a narrow size distribution and have an average diameter of ~18 nm. Figure S4 (Supporting Information) shows a typical TEM image of the PAA-modified $CoFe_2O_4$ nanoparticles. The polymer-coated MNPs remain monodisperse in size with no obvious shape change or aggregation of particles.

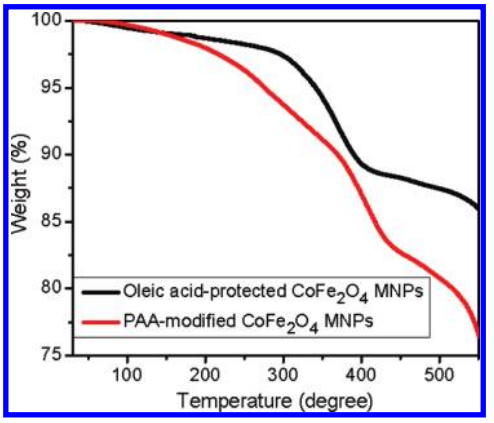

Figure 4. TGA thermogram of $CoFe_2O_4$ MNPs before and after PAA modification.

We became interested in uniform silica coatings around $CoFe_2O_4$ FMNPs ($CoFe_2O_4$@SiO_2) with controlled shell thickness as a method not only to improve the dispersibility of the particles in solution but also to tailor interparticle magnetic coupling interactions, which is known to depend upon the distance between nanoparticles.[17] A critical step toward uniform silica coatings was to transform the hydrophobic (as-synthesized) nanoparticles into hydrophilic PAA-coated MNPs that are soluble in polar ethanolic solutions. Following the formation of the water-soluble PAA-coated $CoFe_2O_4$ MNPs, the Stöber process was employed in order to condense a uniform silica shell onto the MNP surface.[18] Well-defined silica shells were formed around the individual $CoFe_2O_4$ nanoparticles when TEOS was added dropwise to a stirring solution of the PAA-modified $CoFe_2O_4$ nanoparticles. Figure 5b is a typical TEM image of $CoFe_2O_4$@SiO_2 nanoparticles which shows a silica layer with an average thickness of 10 nm was coated uniformly around each MNP, and empty silica particles were not observed. The core diameters of $CoFe_2O_4$@SiO_2 MNPs and the original oleic acid-protected $CoFe_2O_4$ MNPs were identical (18 nm), which indicates that the structure of

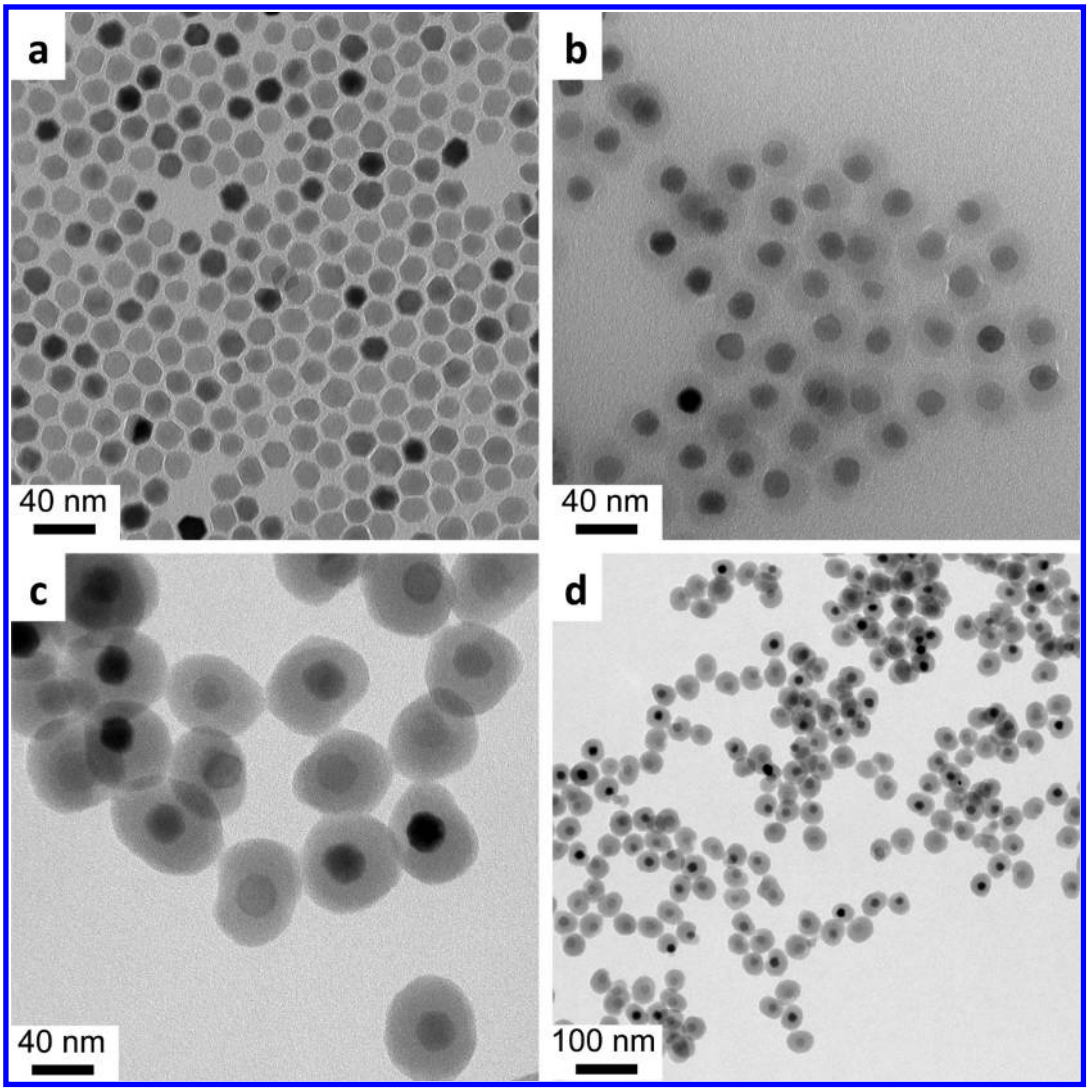

Figure 5. TEM images of the (a) oleic acid-stabilized $CoFe_2O_4$ FMNPs, (b) $CoFe_2O_4$@SiO_2 core−shell particle with a 10 nm shell, and (c, d) $CoFe_2O_4$@SiO_2 core−shell particles with a 20 nm shell.

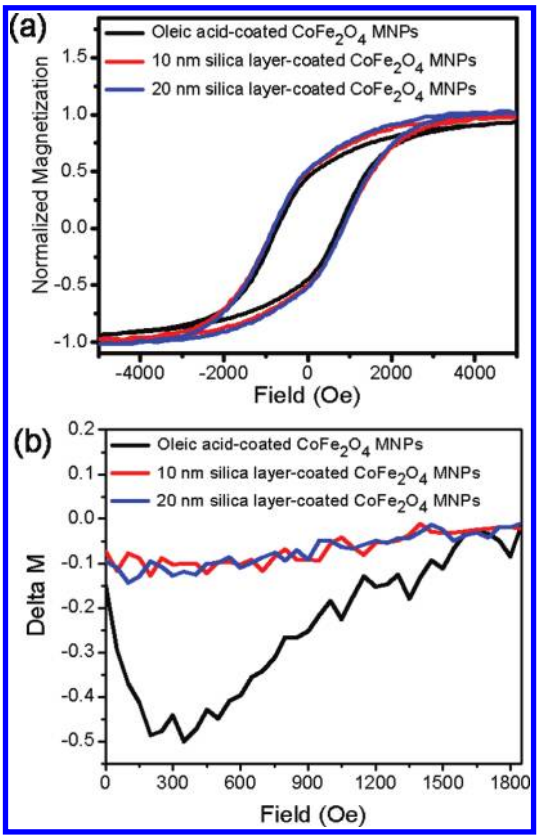

Figure 6. (a) Hysteresis loops measured by VSM (298 K) of the oleic acid-stabilized $CoFe_2O_4$ FMNPs and $CoFe_2O_4$@SiO_2 core−shell particles. (b) ΔM curves for measuring the interparticle magnetic coupling of the oleic acid-stabilized $CoFe_2O_4$ FMNPs and $CoFe_2O_4$@SiO_2 core−shell particles.

MNPs remained intact during the silica coating process. Graf et al. previously reported that if the total surface area of the seed particles per volume is large enough compared to the concentration of TEOS, the formation of new silica particles can be completely suppressed and therefore the thickness of the silica shell can be precisely controlled by the added amount of TEOS.[19] The thickness of silica layer on the particle surface could further be increased to 20 nm by repeated addition of TEOS to a solution of $CoFe_2O_4$@SiO_2 nanoparticle solution, as shown in Figure 5c and 5d. The $CoFe_2O_4$@SiO_2 FMNPs were purified by several washing and magnetic separation steps, which likely removed any empty silica particles that may have formed during the reaction.

In order to study the magnetic behavior of $CoFe_2O_4$ FMNPs before and after silica coating, magnetic hysteresis loops and remanence curves were measured using a vibrating sample magnetometer (VSM) (Figure 6a). The hysteresis loop shows that the 18 nm oleic acid-protected $CoFe_2O_4$ nanoparticles have sufficient magnetocrystalline anisotropy to be ferrimagnetic at 298 K. The coercivity of a random assembly of FMNPs is ~739 Oe, and the saturation of magnetization is 73.6 emu/g, which is in agreement with literature values.[11] The squareness of the hysteresis loop is about 0.45, consistent with a three-dimensional random distribution of the easy axes. The saturation magnetization decreased further to 59.5 emu/g upon coating with a 10 nm silica shell while the coercivity value increased to 832 Oe. The saturation magnetizaton further decreased to 12.6 emu/g, and the coercivity value remained at 832 Oe when the silica shell increased to 20 nm. The reduction of saturation magnetization is a consequence of the increased mass of the nanoparticle associated with the silica shell. Similar results have been observed on the polystyrene-coated $MnFe_2O_4$ MNPs.[7c] The increasing of coercivity is a consequence of the change of the magnetic dipole coupling interaction after silica shell coating. The silica shell encapsulating on the particle surface screens and decreases the magnetic dipole coupling interactions between neighboring MNPs. These observations are consistent with reports from Bertram et al., who reported that strong dipole coupling interaction tends to assist magnetization reversal, thereby reducing the coercivity value from hysteresis loops measurement.[20]

In order to further study the nature of the magnetic dipole coupling interaction between $CoFe_2O_4$ FMNPs, the isothermal remanent magnetization (IRM) and dc demagnetization (DCD) were measured by applying a successively larger field to the initially ac demagnetized sample and a successively larger reverse field to the previously saturated sample. The nature and strength of the magnetic interaction among the particles were determined from the established ΔM technique: $\Delta M = M_d - (1 - 2M_r)$, where M_d is the dc magnetization remanence and M_r is the isothermal remanence. For noninteracting MNPs, ΔM should be zero at any value of applied field. Deviations of ΔM curves from zero are interpreted as a result of magnetic coupling interactions between MNPs.[21] When dipole coupling interaction among the randomly dispersed MNPs are settled, magnetic disorder is induced and the remanent magnetization after saturation is smaller than that corresponding to the initial demagnetized state, leading to $\Delta M < 0$. Figure 6b shows the ΔM curves of $CoFe_2O_4$ MNPs before and after silica coating. A negative peak with a value of −0.5 is present for the oleic acid-protected $CoFe_2O_4$ nanoparticles, indicating a strong dipole coupling interaction between nanoparticles that assists magnetization reversal of the assembly of MNPs. Similar results were reported for ferromagnetic FePt nanoparticles.[22] As shown in Figure 6b, the ΔM peak value becomes −0.1 upon coating the nanoparticles with a 10 and 20 nm silica shell. The change in the ΔM value is a consequence of a reduced magnetic dipole coupling interaction, which depends strongly on interparticle distance. The decreasing of dipole coupling interaction as observed from ΔM curves is also consistent with the increase of coercivity after silica coating as observed from the hysteresis loops. Thus, the silica coating of ferrimagnetic $CoFe_2O_4$ MNPs with controlled shell thickness enables one to tailor the magnetic dipole coupling interactions between the nanoparticles, which is essential to the development of MNP recording media with improved areal density.

Conclusion

In summary, we have successfully developed a method for creating a uniform silica coating of a controlled thickness around individual 18 nm ferrimagnetic $CoFe_2O_4$ nanoparticles. PAA formed complexes with the ferrimagnetic nanoparticles and subsequently ionized to form stable complexes that were readily

(17) (a) Srivastava, S.; Samanta, B.; Arumugam, P.; Han, G.; Rotello, V. M. *J. Mater. Chem.* **2007**, *17*, 52. (b) Boal, A. K.; Frankamp, B. L.; Uzun, O.; Tuominen, M. T.; Rotello, V. M. *Chem. Mater.* **2004**, *16*, 3252. (c) Frankamp, L. B.; Boal, A. K.; Tuominen, M. T.; Rotello, V. M. *J. Am. Chem. Soc.* **2005**, *127*, 9731.
(18) Stober, W.; Fink, A.; Bohn, E. *J. Colloid Interface Sci.* **1968**, *26*, 62.
(19) Graf, C.; Vossen, D. L.; Imhof, A.; Blaaderen, A. V. *Langmuir* **2003**, *19*, 6693.
(20) Chen, X.; Bertram, H. N. *J. Magn. Magn. Mater.* **1992**, *116*, 121.
(21) Franco, V.; Batlle, X.; Labarta, A.; Grady, K. *J. Phys. D: Appl. Phys.* **2000**, *33*, 609.
(22) Zeng, H.; Li, J.; Wang, Z. L.; Liu, J. P.; Sun, S. H. *IEEE Trans. Magn.* **2002**, *38*, 2598.

dispersible. This step was critical to prevent magnetically induced aggregation of the FMNPs by using charge repulsion. The monodisperse particles can be encapsulated with uniform silica shells (with a controlled thickness) around each individual particle. The silica-coated particles form stable dispersions in polar solvents, and the thickness of the oxide shell can tune the interparticle magnetic dipole coupling interaction. This method enables the formation and solution processing of MNPs with tunable magnetic properties for a broad range of magnetic applications including storage and sensors.

Acknowledgment. We thank IBM for funding and support. Work at the Molecular Foundry was supported by the Office of Science, Office of Basic Energy Sciences, of the U.S. Department of Energy under Contract DE-AC02-05CH11231.

Supporting Information Available: Additional VSM characterization, TEM images of the silica-coated superparamagnetic nanoparticles, and photographs of the dispersed $CoFe_2O_4@SiO_2$. This material is available free of charge via the Internet at http://pubs.acs.org.